Engineering Science and Technology, an International Journal 19 (2016) 254–259

HOSTED BY

Contents lists available at ScienceDirect

Engineering Science and Technology, an International Journal

journal homepage: http://www.elsevier.com/locate/jestch

Full Length Article

Enhanced grain refinement of commercial pure copper using the ECAE of Al–Cu–Al tri-layer composite

B. Tolaminejad [a,*], M.M. Hoseini Athar [a], H. Arabi [b], A. Karimi Taheri [c]

[a] Department of Metallurgy and Materials Engineering, Faculty of Engineering, University of Kashan, Kashan, Iran
[b] School of Metallurgy and Materials Engineering, Iran University of Science and Technology, Narmak, Tehran, Iran
[c] Department of Materials Science and Engineering, Sharif University of Technology, Azadi Ave., Tehran, Iran

ARTICLE INFO

Article history:
Received 6 April 2015
Received in revised form
24 July 2015
Accepted 29 July 2015
Available online 1 September 2015

Keywords:
Laminated composite
Equal channel angular extrusion
UFG materials
Aluminum/copper/aluminum

ABSTRACT

Equal channel angular extrusion (ECAE) is a promising technique for production of ultrafine grained (UFG) materials of few hundred nanometers size. In this research, the grain refinement of copper strip is accelerated to ultrafine range by sandwiching it between two aluminum strips and then subjecting the three strips to ECAE process simultaneously. After passing the aluminum–copper–aluminum laminated billet through ECAE die up to 8 passes, tensile properties of the copper layer are evaluated. The optical, scanning and transmission electron microscopes, differential scanning calorimeter, and X-ray diffraction were used to characterize the microstructural changes. The results show that the yield stress of the middle layer (Cu) is increased significantly by about eight times after application of four consecutive passes of ECAE and then it is slightly decreased when more ECAE passes are applied. An ultrafine grain within the range of 150 to 200 nm is obtained in the Cu layer.

Copyright © 2015, The Authors. Production and hosting by Elsevier B.V. on behalf of Karabuk University. This is an open access article under the CC BY-NC-ND license (http://creativecommons.org/licenses/by-nc-nd/4.0/).

1. Introduction

In recent years, the manufacturing of metallic laminated composites using the cold welding processes is highly considered because of their unique and desired mechanical, electrical, and chemical properties [1]. Since a few decades ago, several techniques have been utilized to obtain the cold weld in the mating surfaces of the layers of laminated composites. As an example, one can refer to the application of cold rolling, pressing, and drawing processes in production of cold welded laminated composites [2]. On the other hand, severe plastic deformation (SPD) has recently been developed and passed from the laboratory stage to industrial condition to produce ultrafine grained (UFG) and nano grain size materials [3]. As a SPD process, equal channel angular extrusion (ECAE) is one of the most new methods developed for manufacturing the laminated composites [4,5]. Fig. 1 shows the schematic of ECAE die consisting of an inner angle (φ) and an outer curved corner angle (Ψ). The die is initially charged with a billet inserted in the vertical channel and then pushed into the horizontal channel with the aid of a punch. Under this condition a large strain is induced in the billet, while the cross section of the billet does not experience any change. Eq. (1) presents the equivalent strain imposed on the billet after N passes of ECAE process [6]:

$$\bar{\varepsilon}_N = \frac{N}{\sqrt{3}}\left(2\cot\left(\frac{\varphi+\psi}{2}\right)+\psi\,\mathrm{cosec}\left(\frac{\varphi+\psi}{2}\right)\right) \quad (1)$$

In the past, the cold deformation of laminated composites has been used to create either cold weld between the layers [7–11] or to enhance the workability of a hard metal layer by sandwiching it between two soft layers [12,13]. Also, in some new investigations the hard materials such as titanium (Grade 4) or Al-7075 were deformed by encapsulation aided ECAE without employing back-pressure [14,15]. The mechanical properties and deformation homogeneity of ECA-extruded specimens covered with tube casing are higher than those of the specimens without cover [15]. On the other hand, it is shown that near equi-atomic NiTi shape memory alloys may be successfully processed via ECAE at room temperature by containing the NiTi samples within sheaths [16].

It has been reported [17,18] that equiaxed ultrafine grains of the mean size of approximately 300 nm can be generated in a single copper billet by 12 passes of ECAE. In this research, a further grain refinement of copper strip sandwiched between the aluminum strips was targeted during ECAE process.

* Corresponding author. Tel.: +98 3155913402; fax: +98 3155913402.
E-mail address: tolaminejad@kashanu.ac.ir (B. Tolaminejad).
Peer review under responsibility of Karabuk University.

http://dx.doi.org/10.1016/j.jestch.2015.07.016
2215-0986/Copyright © 2015, The Authors. Production and hosting by Elsevier B.V. on behalf of Karabuk University. This is an open access article under the CC BY-NC-ND license (http://creativecommons.org/licenses/by-nc-nd/4.0/).

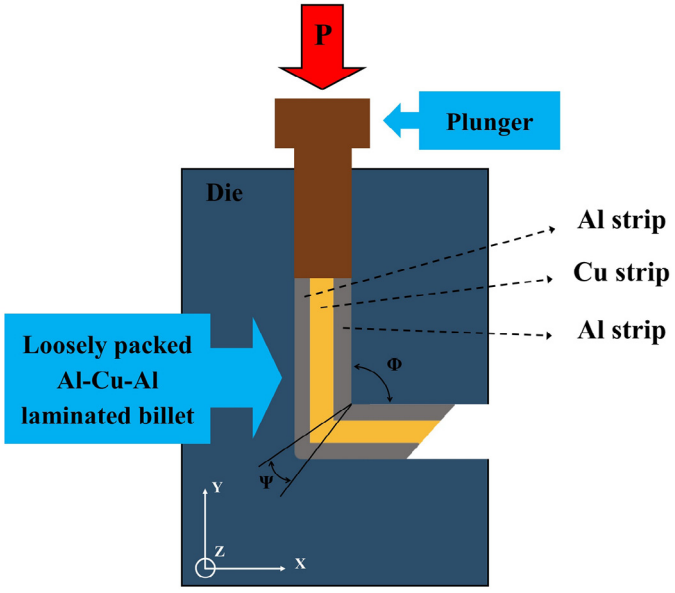

Fig. 1. The schematic of equal channel angular extrusion of Al–Cu–Al laminated billet.

2. Experimental procedures

The materials used in this research consisted of commercial pure copper and aluminum strips and commercial pure copper rod. Copper strips had dimensions of $70 \times 14 \times 5$ mm^3. The aluminum strips had a length of 70 mm, width of 14 mm, and thickness of 4.5 mm. Also, the dimensions of copper billet used as the control or proof specimen were $70 \times 14 \times 14$ mm^3. Degreasing and scratch brushing of the strips' mating surfaces, which is a suitable technique of preparing aluminum/copper/aluminum composite [19], were executed in this work. Then Cu strip was sandwiched between the Al strips. In order to perform the ECAE tests, a split die with an inner angle of $\varphi = 90°$, outer corner angle of $\Psi = 20°$, and a square cross section of 14×14 mm^2 was made. ECAE tests via route B_c (90° clockwise rotation of the specimen after each pass) [20] were carried out up to 8 passes on the composite as well as the copper billet under a constant press velocity of 3 mm/s. In fact, the ECAE force of composite specimen is reduced to less than half of the conventional force for copper billet. The specimen leaving the die is shown in Fig. 2. To study the microstructure of the copper layer in the composite and that of the copper billet after subjecting to different number of passes, specimens with dimensions of $15 \times 5 \times 2$ mm^3 were cut from the ECAE-ed copper billet as well as the copper middle strip. Then, some sections of copper layers parallel to the deformed flow plane were cut from the center of these specimens to study their microstructures. Standard tensile test specimens were machined from the deformed copper billet and the copper strip according to ASTM E-8 standard. These specimens were subjected to tensile test at a strain rate of 10^{-3} s^{-1} using the Instron tensile machine. The fractured surfaces were examined using a Cam Scan MV2300 scanning electron microscope operated at an accelerating voltage of 20 kV. To perform the transmission electron microscopy (TEM) analysis, specimens were prepared through mechanical grinding and twin jet electrolytic polishing in a solution consisting of 250 ml phosphoric acid, 500 ml distilled water, 250 ml ethanol, 50 ml propanol and 5 g urea, at a temperature of –16 °C with conjunction of a voltage of 15 V. TEM micrographs were taken using a Philips CM200 transmission electron microscope operated at 200 kV. Generally, two or three adjacent specimens taken from the center region of flow plane section were analyzed. X-ray diffraction measurement of the extruded copper specimens was carried out on a Philips X pert Pro diffractometer with a Co kα radiation between 20° and 110° using 0.01° per 2 s step size. The volume weighted average domain size (D_v) and the microstrain (ε) were determined using Williamson–Hall relation [21] based on the slope and the ordinate intersection of the line plotted according to the following equation [22]:

$$\left(\frac{\beta Cos\theta}{\lambda}\right) = \frac{1}{D_v} + 2\varepsilon\left(\frac{2Sin\theta}{\lambda}\right) \quad (2)$$

where β, θ and λ are the full-width at half maximum height (FWHM) of the main peaks with maximum intensity (in radian), the Bragg's angle of the peak, and the wave length (in nm), respectively. On the other hand, in the Rietveld method [23], the average dislocation density (ρ) can be estimated from the relation $\rho = (\rho_d \cdot \rho_s)^{1/2}$ where, $\rho_d = 3/D_v^2$ (dislocation density due to the domain), $\rho_s = \langle \varepsilon^2 \rangle / b^2$ (dislocation density due to the microstructure), and b is the Burgers vector. For differential scanning calorimetry (DSC) experiments, the samples were cut into a disc 3 mm in diameter and 0.9 mm in height. These experiments were carried out using a Dupant 2000 unit in a temperature range of 50–350 °C at a constant heating rate of 10 °C/min and using high purity Ar gas to assess the variation in recovery temperature in the Cu strip as well as Cu billet after deformation by ECAE process.

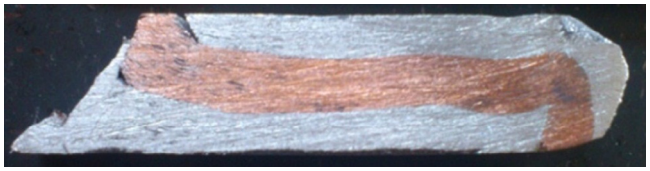

Fig. 2. Tri-layer specimen after four ECAE passes.

3. Results and discussion

The optical examination of the samples prior to the ECAE process indicated that copper strip consisted of equiaxed grain structure (Fig. 3a). The microstructure of this specimen after one pass of ECAE has been shown in Fig. 3b. As it is seen, the original grains are uniformly elongated at an angle of about 26° to extrusion axis. Fig. 3c represents the microstructure of the specimen after 4 passes of ECAE. This figure exhibits an intensive fragmentation of the pan-cake or fibrous structure, which is typically formed during the early passes of ECAE. By increasing the number of passes, the original structure has fairly been restored as refined equiaxed grains at fourth pass based on route B_c mechanism. This phenomenon is justified as the rotation of the samples by +90°, which causes the shearing of the deformed grain on two orthogonal planes in reverse direction. It is noted that the appropriate strain for restoration of equiaxed grains after being elongated by ECAE was achieved by four passes. The shear strains generating at the first four passes are ε_{xz} at the first pass; $(\varepsilon_{xz} + \varepsilon_{yz})$ at the second pass; ε_{yz} at the third pass and (0) for the fourth pass [24].

Referring to Fig. 4, it is seen that the yield stress of the deformed proof and of copper layer of the ECAE-ed laminated composite is significantly increased after one pass of ECAE, so that the yield stress becomes nearly seven times of the initial yield stress. However, the rate of increase in the yield stress in the subsequent three passes is decreased substantially. Beyond the fourth pass, the yield stress is slightly reduced. Fig. 5 represents typical fracture surfaces of the copper layer in proof and composite specimens. As it is observed, the secondary electron image (SEI) fractograph of the deformed copper shows a large amount of dimples which is an indication of

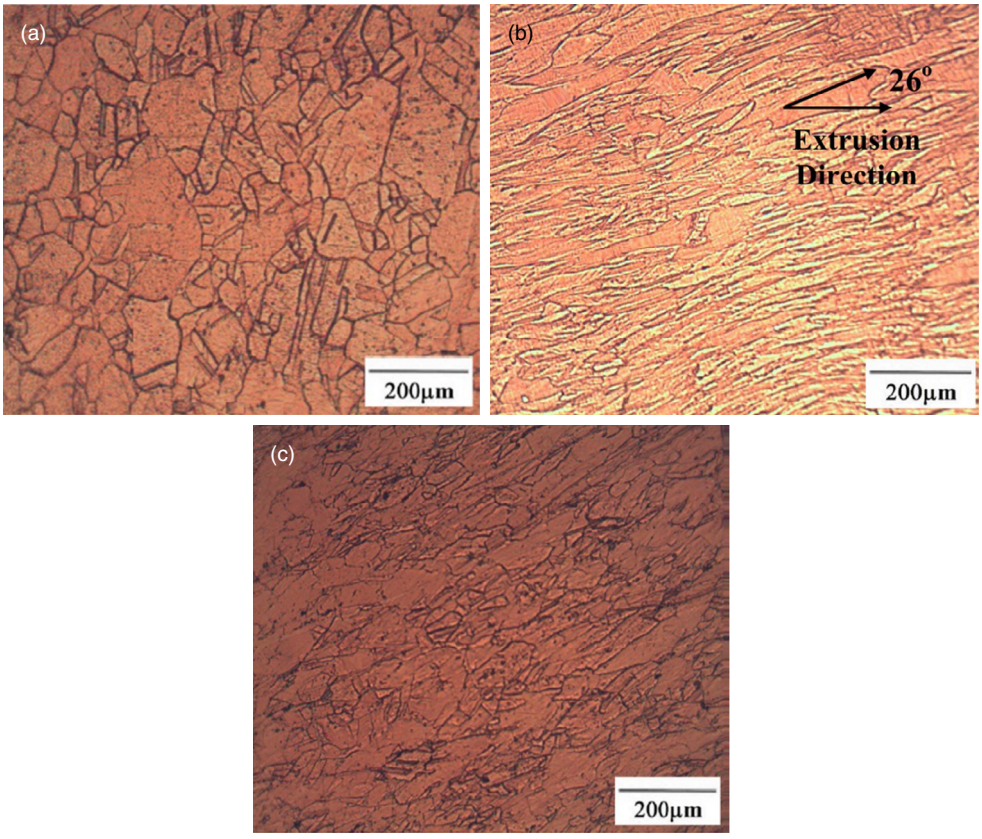

Fig. 3. Optical micrographs of the copper specimens (a) annealed, (b) 1 pass, (c) 4 passes.

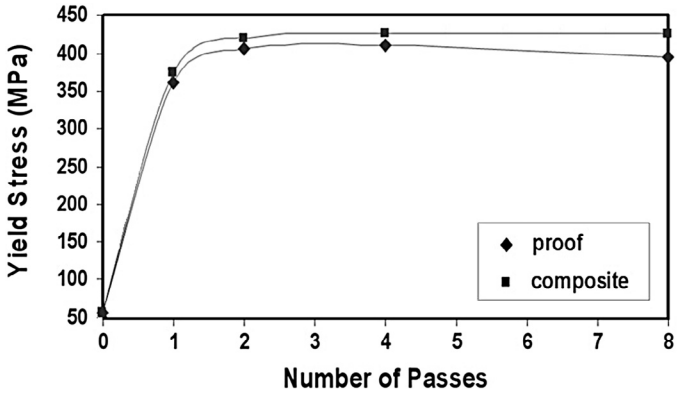

Fig. 4. Effect of the number of passes (i.e. equivalent to the amount of increase in deformation strain) on the yield stress of copper: proof and composite specimens.

a transgranular ductile behavior. There is also an inhomogeneous distribution of dimple sizes between 3 μm and 30 μm found especially in the fractograph surface of the composite specimen.

Fig. 6 demonstrates the variations of dislocation density as a function of the number of passes of ECAE process. The dislocation density increases from 1.3×10^{14} to ~$25.1 \times 10^{14}/m^2$ in composite specimen when the strain increases from 0 to about 4.3 (equivalent to four passes of ECAE). However, this density is decreased during further deformation particularly in proof specimen. It is shown that in contrast with the mentioned variations, no reduction can be observed in the yield strength, even beyond 4 passes in composite specimen (Fig. 4). This trend is probably related to the strengthening compensation via grain boundary mechanism due to the continuous grain refinement related to the appearance of the characteristics of strain hardening stage IV and the disappearance

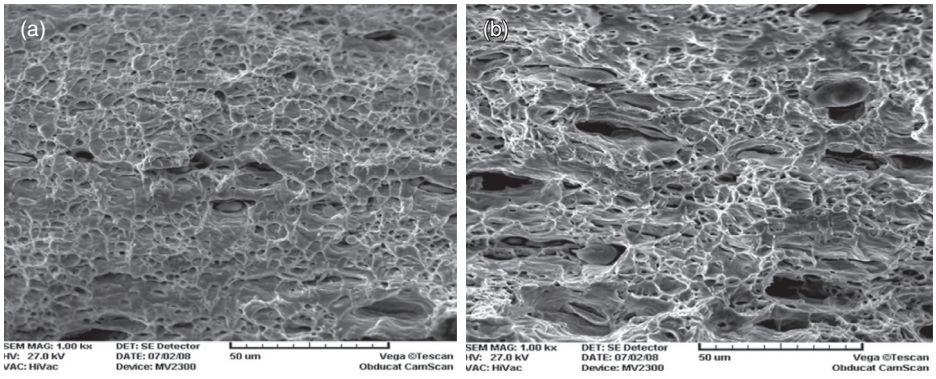

Fig. 5. Fracture surface of the copper layer ECA-extruded in different conditions: (a) proof specimen and (b) composite specimen.

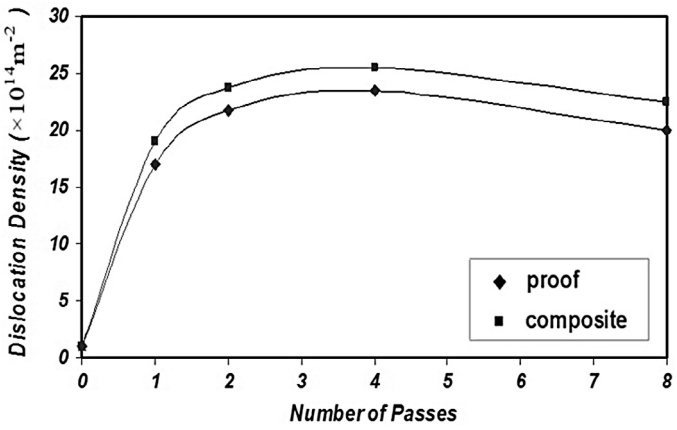

Fig. 6. Variations of dislocation density of copper layer with the number of passes: proof and composite specimens.

of dislocation mechanism related to strain hardening stage III reported by Hansen et al. [25]. Thus, the distribution of bimodal large and deep dimples accompanied by small dimples in the fracture surface (Fig. 5b) probably indicates that considerable deformation energy has been expended by a process of void coalescence.

The strain softening phenomenon occurs due to dislocations rearrangement by increasing the number of ECAE passes up to 4. This phenomenon decreases the increasing rate of mobile dislocation density (Fig. 6) as a result of annihilation process, formation of locks, and the formation of dipoles [26]. In the steady state condition, the density of dislocations, ρ, can be expressed as follows [27]:

$$\rho = \frac{\alpha \dot{\varepsilon} \tau}{bd} \tag{3}$$

By substituting the calculated values of ρ and the average grain size, d, and taking b = 0.255 nm, $\dot{\varepsilon} = 10^{-3}$ s^{-1}, and α = 2.4, the relaxation time, τ, for dislocation absorption in grain boundaries is estimated to be about 12 s for copper subjected to 4 passes. Also, for this UFG sample, the deformation time was about 150 s. Thus, the time for dislocation absorption in grain boundaries is less than the deformation time. This may lead to lack of dislocation accumulation and the absence of strain hardening during tension test of ECAE processed commercially pure Cu.

According to Fig. 7, the DSC heat flow traces of each copper specimen appear as an exothermic peak corresponding to the recovery of microstructure [28]. The maximum of the peak has shifted to lower temperature values and the released heat is significantly increased with increase in the number of passes up to 4th pass. These changes may be attributed to the increase in stored energy being mainly in the form of elastic energy in the strain fields of dislocations and point defects. The introduced stored energy by severe plastic deformation raises the driving force for nucleation of new strain-free grains, meaning that the formation of new cells and grains are activated at lower temperatures [29,30]. In fact, as it is seen in proof specimen, the DSC peaks between four and eight passes

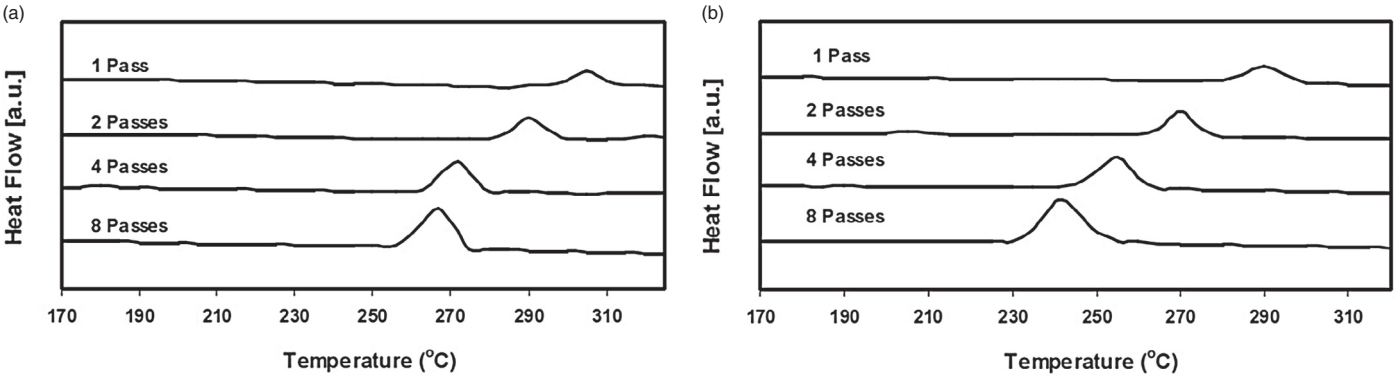

Fig. 7. Differential scanning calorimetric curves showing the variation of recovery temperature: (a) the proof specimen and (b) composite specimen after 1 to 8 passes of ECAE.

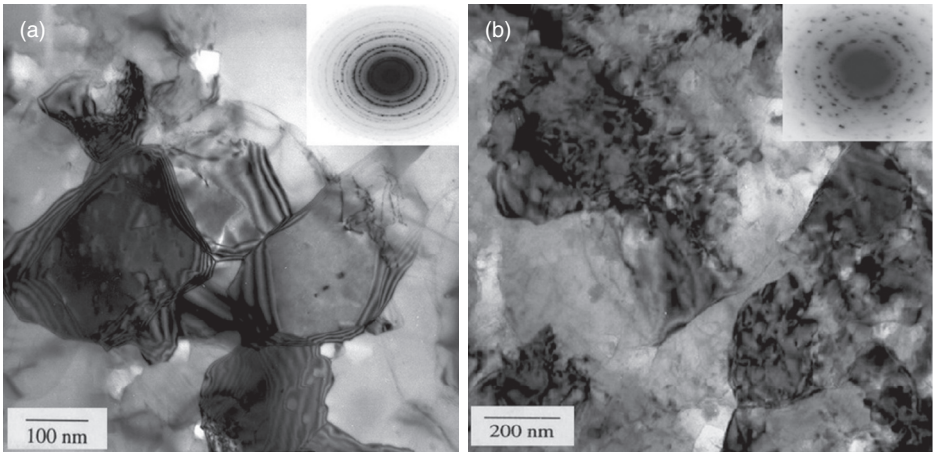

Fig. 8. TEM micrographs and SAED pattern of copper: (a) proof specimen and (b) composite specimen after 4 passes.

Table 1
The average copper grain size obtained using different techniques.

Number of passes applied	Average cell size D_w (nm) determined by TEM technique		Average cell size D_c (nm) determined by XRD technique		Average cell size (nm) calculated	
	Proof	Composite	Composite	Proof	Composite	Proof
2	250	215	59	70	220	245
4	235	190	48	56	200	230
8	215	165	44	54	175	220

elucidate no considerable shift to lower temperature compared to the peaks corresponding to composite specimen. This difference may be ascribed to the observation that the materials encapsulated with soft cartridge are generally more easily ECA-extruded than the base material as reported by Li et al. [14]. Also, Arnold and Whitton [12] and Atkins and Weinstein [13] obtained more workability of a hard metal strip by sandwiching it between two soft strips before rolling and compression, respectively. These researchers have emphasized that a prerequisite of deformation process of the laminated composites is the transmission of shear stresses setting up the redistributed tensile and compressive stresses in composite layers.

Fig. 8 shows the microstructure and the associated selected area electron diffraction (SAED) pattern of {111} planes with respect to the specimens after 4 passes of ECAE. As can be observed from the figure, the microstructure of copper in composite specimen consists of equiaxed ultrafine grains of ≈150–200 nm in diameter and poorly delineated grain boundaries, with fringed structure (Fig. 8a). It has been reported that the sharp boundaries with grain interior almost free from dislocation are an indication of low internal stress in non-equilibrium grain boundaries by prevailing the trapped lattice dislocations (TLDs) [31,32].

It is interesting to note that whereas the composite specimen has a set of ring selected area diffraction, the diffraction pattern of proof specimen is not well defined (Fig. 8b). To evaluate the average size of dislocation cells and subgrains developed during deformation, the following procedures may be used.

The value of yield strength of an UFG material has been determined using the strengthening models according to Lian et al. [33]. In the model, the plastic flow is considered to be controlled by the stress required to attain dislocation within a set of larger grains of semicircle configuration. The critical stress to activate the Frank-Read source [34] in such configuration has been presented as:

$$\sigma = \frac{MGb}{2\pi L(1-\nu)}\left[\left(1-\frac{3\nu}{2}\right)\ln\left(\frac{L}{b}\right)-1+\frac{\nu}{2}\right] \quad (4)$$

where, M is the Taylor factor which is assumed to be equal to 3.06 for a polycrystalline FCC material of random orientation, G is the shear modulus, b is the Burgers vector, υ is Poisson's ratio, and L is the average spacing of dislocations which depends on dislocation density $\left(L=\frac{1}{\sqrt{\rho}}\right)$ [35]. According to this method, the average spacing of dislocation can be calculated by substituting the above microstructural variables such as M, G and υ for copper and the measured yield strength into Eq. (4). Then, by calculating L from this equation, the ρ can be obtained. Thereafter, the average copper cell size related to different ECAE passes can be determined as below.

Two strengthening mechanisms may contribute to strengthening during the large deformation of materials. The first is the mechanism of dislocation strengthening due to presence of incidental dislocation boundaries (IDBs) of small misorientation. These boundaries arise from the statistical trapping of dislocations. The second mechanism is the grain boundary strengthening via Hall–Petch relationship due to formation of geometrically necessary boundaries (GNBs) arising from the difference in the slip system operating in the neighboring slip systems or the local strain difference within each grain and it is composed of high angle grain boundaries at large strain. The proposed strengthening equation utilized in several recent researches on UFG materials [25,27] is expressed as:

$$\sigma = \sigma_0 + M\alpha Gb\sqrt{\rho} + \frac{k}{\sqrt{d}} \quad (5)$$

where σ_0 is the friction stress, α is a constant, d is the average grain size, and k is the Hall–Petch constant. By substituting the value of variables (i.e., σ, σ_0, m, α, and k) and the value of ρ obtained from Eq. (4) into Eq. (5), one can calculate the developed cell size during ECAE process. The calculated values for different specimens have been compared with those obtained from the XRD and TEM studies in Table 1. The TEM measured cell size is approximately three to four times greater than the coherent domain size determined by XRD. This difference may be attributed to the characteristics of each technique of measurement. It should be considered that the coherent scattering length of the lattice, which is limited by the lattice defects such as dislocation tangles, can be detected by X-ray diffraction and taken as an independent (sub)grain, while the micrographs obtained by TEM are only credited when they are taken from a specific direction. Thus, it seems that some of the cell wall has not been visible when the TEM technique has been used [18].

During the ECAE process, the low angle boundaries of an average distance of D_c are extended along the layers of high angle grain boundaries of an average spacing of D_b as proposed by Petryk and Stupkiewicz [36]:

$$\sigma_y = \sigma_1 + (1-\xi_h)k_c Gb\frac{1}{D_c} + \xi_h k_b \frac{1}{\sqrt{D_b}} \quad (6)$$

D_b and D_c were obtained using the XRD and TEM results, respectively and substituted into Eq. (6). Then, based on the constant values in Table 2, the high angle grain boundary area fraction (ξ_h) was calculated (Fig. 9). Although there is no increase in dislocation density between 4 and 8 passes (Fig. 6), at the same time based on the calculated results, the grain boundary orientation changes even between four and eight passes. Accordingly, the operative slip systems may be affected on a microscopic level to change the resulting texture leading to more refinement [38].

The FEM simulation may be helpful to evaluate accurately the deformation mechanics of a tri-layer composite. Furthermore, one may assess the microtexture and grain boundary character distribution (GBCD) due to their primary roles in microstucture

Table 2
Mechanical and physical constants of copper [37] used in Eq. (6).

B (nm)	σ_1 (MPa)	k_c	k_b (MPaμm$^{1/2}$)	G (GPa)
0.255	3.4	1.5	176	46

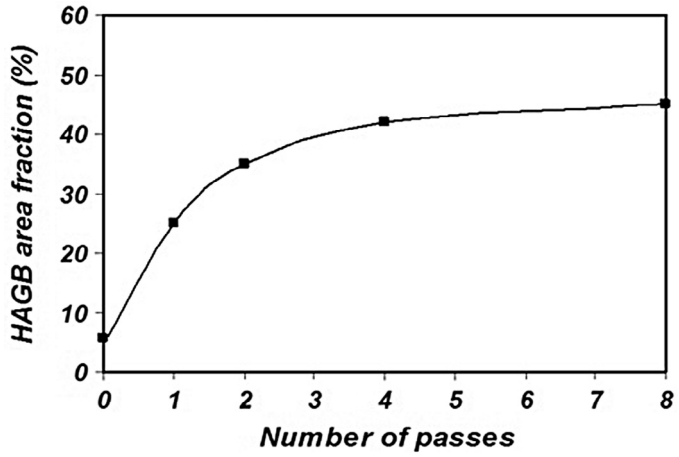

Fig. 9. Variations of HABs area fraction of copper layer versus number of ECAE passes performed on composite specimens.

development. For the sake of brevity it is not possible to present the simulation and EBSD results in this paper. They will be presented elsewhere.

4. Conclusions

In the present research, the tri-layer aluminum–copper–aluminum strips were ECA-extruded. The yield stress and the grain size of the copper middle layer were evaluated and compared with those of a mono copper billet extruded at the same conditions. The results show that the ECAE process increases the copper yield stress up to eight times and the rate of increase in strength is significantly decreased after the first pass and becomes insignificant or weak after the fourth pass.

XRD analysis accounts a rather large fraction of sub-boundaries, which were not included in the TEM analysis. Thus some differences were seen in the microstructural parameters measured by TEM and XRD, though the results obtained by these two techniques were qualitatively in good agreement.

A finer grain size can be achieved at a smaller number of passes in copper strip by sandwiching it between two Al strips and then ECA-extruding the sandwich billet. The method introduced in this research is very useful for the ECAE process of high-strength alloys requiring high extrusion force.

Acknowledgements

The authors would like to thank the Research Board of Sharif University of Technology, Tehran, Iran for the provision of the research facilities used in this work.

References

[1] R.F. Tylecote, Investigation on pressure welding, Br. Weld. J. 5 (1994) 117–134.
[2] P.K. Wright, D.A. Snow, C.K. Tay, Interfacial conditions in cold pressure welding, Metals Technol. 5 (1) (1978) 24–31.
[3] V.M. Segal, Materials processed by simple shear, Mater. Sci. Eng. A. 197 (1995) 157–164.
[4] A.R. Eivani, A. Karimi Taheri, A new method for producing bimetallic rods, Mater. Lett. 61 (2007) 4110–4113.
[5] X.B. Liu, R.S. Chen, E.H. Han, Preliminary investigations on the Mg–Al–Zn/Al laminated composite fabricated by equal channel angular extrusion, J. Mater. Process. Technol. 209 (2009) 4675–4681.
[6] Y. Iwahashi, J. Wang, Z. Horita, M. Nemoto, T.G. Langdon, Principles of equal channel angular pressing for processing of ultra-fine grained materials, Scr. Mater. 35 (1996) 143–146.
[7] H.W. Wagener, J. Haats, Pressure welding of corrosion resistant metals by cold extrusion, J. Mater. Process. Technol. 45 (1994) 275–280.
[8] A. Karimi Taheri, Analytical study of drawing of non-bounded tri metallic strips, Int. J. Mech. Tools Manufac. 33 (1) (1993) 71–78.
[9] H. Danesh Manesh, A. Karimi Taheri, An investigation of deformation behavior and bonding strength of bimetal strip during rolling, Mech. Mater. 37 (5) (2005) 531–542.
[10] H. Danesh Manesh, A. Karimi Taheri, Bond strength and formability of an aluminum-clad steel sheet, J. Alloys Compd. 361 (1–2) (2003) 138–143.
[11] B. Tolaminejad, H. Arabi, A study of roll bonding MS90 alloy to steel utilizing chromized interlayer, Iran. J. Sci. Technol. B. 32-B6 (2008) 631–640.
[12] R.R. Arnold, P.W. Whitton, Stress and deformation studies for sandwich rolling hard metals, Proc. Inst. Mech. Eng. 173 (1959) 241–256.
[13] A.G. Atkins, A.S. Weinstein, The deformation of sandwich materials, Int. J. Mech. Sci. 12 (1970) 641–657.
[14] Y. Li, H.P. Ng, H.-D. Jung, H.-E. Kim, Y. Estrin, Enhancement of mechanical properties of grade 4 titanium by equal channel angular pressing with billet encapsulation, Mater. Lett. 114 (2014) 144–147.
[15] M.H. Shaeri, F. Djavanroodi, M. Sedighi, S. Ahmadi, M.T. Salehi, S.H. Seyyedein, Effect of copper tube casing on strain distribution and mechanical properties of Al-7075 alloy processed by equal channel angular pressing, J. Strain Anal. Eng. 48 (8) (2013) 512–521.
[16] H. Shahmir, M. Nili-Ahmadabadi, M. Mansouri-Arani, T.G. Langdon, The processing of NiTi shape memory alloys by equal-channel angular pressing at room temperature, Mater. Sci. Eng. A. 576 (2013) 178–184.
[17] V.I. Kopylov, V.N. Chuvil'deev, in: Proceedings of Nato Advanced Study Institute on Nanostructured Materials by High-pressure Severe Plastic Deformation, Nato Science Series II, Netherlands, 2006, paper # 69–76.
[18] F.D. Torre, R. Lapovok, J. Sandlin, P.F. Thomson, C.H.J. Davies, E.V. Pereloma, Microstructures and properties of copper processed by equal channel angular extrusion for 1-16 pass, Acta Mater. 52 (2004) 4819–4832.
[19] W. Zhang, N. Bay, Cold welding-experimental investigation of the surface preparation methods, Weld. Res. Suppl. 76 (8) (1997) 326–330.
[20] R.Z. Valiev, T.G. Langdon, Principles of equal-channel angular pressing as a processing tool for grain refinement, Prog. Mater. Sci. 51 (2006) 881–981.
[21] G.K. Williamson, W.H. Hall, X-ray line broadening from filed aluminium and wolfram l'elargissement des raies de rayons x obtenues des limailles d'aluminium et de tungstenedie verbreiterung der roentgeninterferenzlinien von aluminium-und wolframspaenen, Acta Metall. 1 (1953) 22–31.
[22] P. Mukherjee, A. Sarkar, P. Barat, S.K. Bandyopadhyay, S. Pintu, S.K. Chattopadhyay, Deformation characteristics of rolled zirconium alloys: a study by x ray diffraction line profile analysis, Acta Mater. 52 (2004) 5687–5696.
[23] G.K. Williamson, R.E. Smallman, Dislocation line broadening, Philos. Mag. 1 (1956) 34–46.
[24] A. Gholinia, P.B. Prangnell, M.V. Markushev, The effect of strain path on the development of deformation structures in severely deformed aluminum alloys processed by ECAE, Acta Mater. 48 (2000) 1115–1130.
[25] N. Hansen, X. Huang, D.A. Hughes, Microstructural evolution and hardening parameters, Mater. Sci. Eng. A. 317 (2001) 3–11.
[26] M. Goerdeler, G. Gottstein, A microstructural work hardening model based on three internal state variables, Mater. Sci. Eng. A. 309–310 (2001) 377–381.
[27] Y.G. Ko, D.H. Shin, K.-T. Park, C.S. Lee, An analysis of the strain hardening behavior of ultra-fine grain pure titanium, Scr. Mater. 54 (2006) 1785–1789.
[28] J. Gubicza, L. Balogh, R.J. Hellmig, Y. Estrin, T. Ungar, Dislocation structure and crystallite size in severely deformed copper by X-ray peak profile analysis, Mater. Sci. Eng. A. 400–401 (2005) 334–338.
[29] Y.M. Wang, E. Ma, Three strategies to achieve uniform tensile deformation in a nanostructured metal, Acta Mater. 52 (2004) 1699–1709.
[30] R.W.K. Honeycombe, The Plastic Deformation of Materials, second ed., Edward Arnold Publishers, London, 1984.
[31] W. Lojkowski, On the spreading of grain boundary dislocations and its effect on grain boundary properties, Acta. Metall. Mater. 39 (8) (1991) 1891–1899.
[32] A.A. Nazarov, A.E. Romanov, R.Z. Valiev, Incorporation model for the spreading of extrinsic grain boundary dislocations, Scr. Metall. Mater. 24 (1990) 1929–1934.
[33] J. Lian, B. Baudelet, A.A. Nazarov, Model for prediction of the mechanical behaviour of nanocrystalline materials, Mater. Sci. Eng. A. 172 (1993) 23–29.
[34] J.P. Hirth, J. Lothe, Theory of Dislocations, second ed., John Wiley & Sons, New York, 1982.
[35] D. Kuhlmann-Wilsdrof, Theory of plastic deformation: properties of low energy dislocation structures, Mater. Sci. Eng. A. 113 (1989) 1–41.
[36] H. Petryk, S. Stupkiewicz, A quantitative model of grain refinement and strain hardening during severe plastic deformation, Mater. Sci. Eng. A. 444 (2007) 214–219.
[37] A.W. Thomson, M.I. Baskes, W.F. Flanagan, The dependence of polycrystal work hardening on grain size, Acta Metall. 21 (1973) 1017–1028.
[38] P.L. Sun, P.W. Kao, C.P. Chang, High angle boundary formation by grain subdivision in equal channel angular extrusion, Scr. Mater. 51 (2004) 565–570.